J. Membrane Biol. 64, 77–89 (1982)

The Journal of
Membrane Biology

The Role of Sodium-Channel Density in the Natriferic Response of the Toad Urinary Bladder to an Antidiuretic Hormone

Jack H.-Y. Li, Lawrence G. Palmer*, Isidore S. Edelman, and Bernd Lindemann

II. Physiologisches Institut der Universität des Saarlandes, D 6650 Homburg/Saar, West Germany,
and Department of Biochemistry, College of Physicians and Surgeons, Columbia University, New York, New York

Summary. Urinary bladders of *Bufo marinus* were depolarized, by raising the serosal K concentration, to facilitate voltage-clamping of the apical membrane. Passive Na transport across the apical membrane was then studied with near-instantaneous current-voltage curves obtained before and after eliciting a natriferic response with oxytocin. Fitting with the constant-field equation showed that the natriferic effect is accounted for by an increase in the apical Na permeability. It is accompanied by a small increase in cellular Na activity. Furthermore, fluctuation analysis of the amiloride-induced shot-noise component of the short-circuit current indicated that the permeability increase is not due to increased Na translocation through those Na channels which were already conducting prior to hormonal stimulation. Rather, the natriferic effects is found to be based on an increase in the population of transporting channels. It appears that, in response to the hormone, Na channels are rapidly "recruited" from a pool of electrically silent channels.

Key words transepithelial Na transport · apical Na permeability · Na-channel density · oxytocin

Introduction

One of the physiological effects of antidiuretic hormone[1] in amphibia is a natriferic response of the target epithelial (e.g., Fuhrman & Ussing, 1951). The stimulation of Na uptake is apparently achieved predominantly through an increase in Na permeability of the apical membrane (Curran, Herrera & Flanigan, 1963), mediated by a raised cellular concentration of cyclic AMP (e.g., Orloff & Handler, 1962, 1967).

This paper deals with the nature of the hormone-controlled increase in Na permeability in the urinary bladder of *Bufo marinus*. Three possibilities are considered: (i) The stimulation is achieved by an increase in single-channel Na conductance, (ii) the mean open-time of the channels is increased, as suggested by Cuthbert and Shum (1974), or (iii) The single-channel current and the open-close switching rates remain unchanged, but more channels are made available for transport. We verified by means of near-instantaneous current-voltage curves that in the depolarized state the preparations respond to oxytocin with an increase in apical Na permeability. We then used the amiloride-induced shot-noise technique of Lindemann and Van Driessche (1977) to analyze single-channel currents and area densities of channels before and after hormonal stimulation.

The results indicate that the properties of individual channels, including the magnitude of the single-channel current and the sensitivity to block by amiloride and by Na, are not substantially changed. The increase in P_{Na} is accounted for by an increase in the area density of conducting channels.

Our results were reported at the 1979 fall meeting of the Deutsche Physiologische Gesellschaft (Li, Palmer, Edelman & Lindemann, 1979).

Abbreviations and Definitions

I_{sc}	Short-circuit current (i.e., at $V=0$)
I_{Na}	Transcellular, amiloride-inhibitable Na-current per μF apical capacitance
V	Transepithelial voltage
P_{Na}	Amiloride-inhibitable Na permeability of the apical membrane
P_{max}	Na permeability of the apical membrane at $A_o=0$ and $Na_o=0$ [found by extrapolation, *see* Eq. (1)]
P'_{max}	Na permeability of the apical membrane at $A_o=0$ and $Na_o=60$ mM
Na_o	Mucosal Na activity
Na_c	Na activity of the cytoplasm obtained by I_{Na}–V curves. Na_c represents the activity at the apical cell pole close to the Na channels
A_o	Amiloride concentration in the mucosal solution

* *Present address:* Department of Physiology, Cornell University Medical College, New York, New York 10021.

[1] Vasopressin and vasotocin are the neurohypophyseal peptides that have been identified as antidiuretic hormones, in mammals and anurans, respectively. In the toad bladder, oxytocin also elicits an antidiuretic response. For practical reasons oxytocin was used in our study of the natriferic effects of these hormones.

0022-2631/82/0064/-0077 $02.60

K_N	Apparent inhibition constant or disociation constant of the block of P_{Na} by mucosal Na ions
K_A^{ma}	Apparent inhibition constant of the block of Na channels by amiloride, obtained by macroscopic measurements (dose-response curves)
K_A	Microscopic inhibition constant of amiloride ($=k_{20}/k_{02}$) in the absence of competitive inhibitors
K'_A	Apparent microscopic inhibition constant of amiloride, obtained from shot-noise analysis as k'_{20}/k'_{02}
k'_{20}, k'_{02}	Apparent off- and on-rate constants of the blocking event as obtained from plots of $2\pi f_c^A$ *vs.* A_o (rate-concentration plots). The constants include the Na-amiloride competition effect as described in Appendix A.
PDS	Power density spectrum. The units $A^2 \cdot s$ used are understood as A^2/Hz
f_c^A	Corner frequency (frequency at half plateau power) of the amiloride-induced Lorentzian shot-current PDS
G_0	Low frequency plateau of the amiloride induced shot-current PDS
r_2	"Chemical rate" or inverse relaxation time constant of the amiloride-dependent blocking action: $2\pi f_c^A \simeq k_{02} A_o + k_{20}$
i	Shot-current (change in channel current) caused by random block of a Na channel by amiloride. For channels with only two conductive states in which amiloride causes a full block, i will be identical with the single-channel Na current
$\bar{i}$	Average of i values obtained at all amiloride concentrations used
P_0	Probability for a channel to remain open in the presence of amiloride and mucosal Na
P_1	Probability for a channel to be blocked by mucosal Na
P_2	Probability for a channel to be blocked by amiloride
N_0	Area density of conducting Na channels. Values are given per μF or per 10 fF of apical membrane capacitance, corresponding approximately to 1 cm^2 and 1 μm^2 of membrane area, respectively
N_1	Area density of channels blocked by mucosal Na
N_2	Area density of channels blocked by amiloride
N	Total density of electrically detectable Na channels ($=N_0+N_1+N_2$)
N_x	Pool of Na channels of unknown location which can be "recruited" to become electrically detectable
SEM	Standard error of the mean
SD	Standard deviation
r	Regression coefficient

Materials and Methods

Bufo marinus of Mexican origin (obtained from Lemberger, Wisc.) were kept at room temperature in tanks with free access to tap water. The urinary bladders were removed and mounted as moderately stretched flat sheets im Lucite chambers having a cross-sectional area of 3 cm^2. The mucosal solution was constantly renewed by gravity feed, keeping the mucosal compartment at a hydrostatic pressure 10 cm higher than that of the serosal side. Thus the tissue was flattened against a filter-paper support on its serosal side, minimizing microphonics due to tissue movement. The tissue edge was protected from mechanical trauma by an undercured silicon washer facing the mucosal side (for further details *see* Palmer, Edelman & Lindemann, 1980). All experiments were carried out at room temperature.

Mucosal solutions contained Na_2SO_4 plus K_2SO_4 at a constant combined concentration of 54.5 mM (Na activity coefficient of 0.55), 1 mM Ca-gluconate and 5 mM Tris-H_2SO_4, pH 7.5 (*see* Fuchs, Hviid Larsen & Lindemann, 1977). The Na activity (Na_o) was varied by replacement with K to maintain the ionic strength constant. The mucosal solutions were slightly hypotonic with respect to the serosal solution. For I-V measurements, Na_o did not exceed 20 mM activity; for noise measurements it was kept at 60 mM activity. Stock solutions of 8 mM amiloride (a gift of Merck, Sharp & Dohme) were made with deionized water. From these, aliquots were added to the mucosal solutions to final concentrations between 0.5 and 80 μM. The serosal solution consisted of (in mM): 85, KCl; 50, sucrose; 1, $CaCl_2$; 0.5, $MgSO_4$; 3.5, K-phosphate (pH 7.5); and 5, glucose. It was applied for at least 1 hr prior to measurements. As shown by Palmer et al. (1980), this solution depolarizes the basal-lateral membrane potential and decreases the basal-lateral membrane resistance, as expected for a membrane of high K-permeability. During K depolarization a transepithelial voltage clamp should control the voltage of the apical membrane as long as the cellular Na concentration remains small. Oxytocin (Sigma) was added to the serosal solution to a final concentration of 60 mU/ml, which elicits a maximal natriferic response.

Apical membrane area was estimated by measurement of tissue capacitance from the voltage response to rectangular current pulses (Palmer et al., 1980). For these measurements the epithelia were serosally depolarized with the KCl-sucrose medium, while the mucosal sulfate solution contained a maximally inhibitory concentration of amiloride or was free of Na. The capacitance measurements were checked occasionally by recording impedance spectra from 0.1 to 2000 Hz with a sine-wave burst method (Warncke & Lindemann, 1979).[2] The agreement was satisfactory. Typically, the apical capacitance was approximately 6 μF in chambers of 3 cm^2 cross-sectional area at moderate stretch of the bladder. The impedance method permits simultaneous estimation of apical and basal-lateral membrane capacitances and resistances. Warncke and Lindemann (1980) found that the KCl-sucrose medium decreased the slope resistance in parallel to the larger membrane capacitance (i.e., the basal-lateral resistance) to values of less than 50 Ω for each μF of apical capacitance.

Near-instantaneous I-V curves were recorded by transepithelial voltage-clamping, using a staircase-shaped sequence of command voltage pulses of 2 to 10 msec step length, and except where indicated, 5 mV step amplitude (Fuchs et al., 1977; Palmer et al., 1980). The resulting clamp currents were sampled by a computer and plotted against the corresponding voltage. The shunt I-V curves were obtained after adding 80 μM amiloride to the mucosal solution, or after replacing Na_o by K and waiting for decay of the resulting outward-current transient. Under steady-state conditions in the presence of 80 μM amiloride or with the Na-free solution on the mucosal side, the short-circuit current (I_{sc}) was small in magnitude and usually negative (i.e., reversed). After measurement of the steady-state shunt I-V curves, the mucosal solutions were replaced with fresh 20 mM Na_o followed by a series of solutions of progressively lower Na activities (i.e., 20 to 5 mM). An I-V curve was generated at each activity after a steady state was reached, usually 2 to 3 min after the change of solution. In these cases a single shunt I-V curve, taken either just before or after the Na series, was used to correct the curves obtained at all Na activities by current subtraction. Sometimes the sequence was reversed, using steps of increasing Na activity. Occasionally, the shunt I-V curves were recorded soon after exposure to each Na_o, in the presence of 80 μM amiloride added to the Na-containing mucosal solution. The three protocols gave similar results.

In each analysis three parameters were calculated by the

[2] We thank Dr. J. Warncke for measuring the impedance spectra.

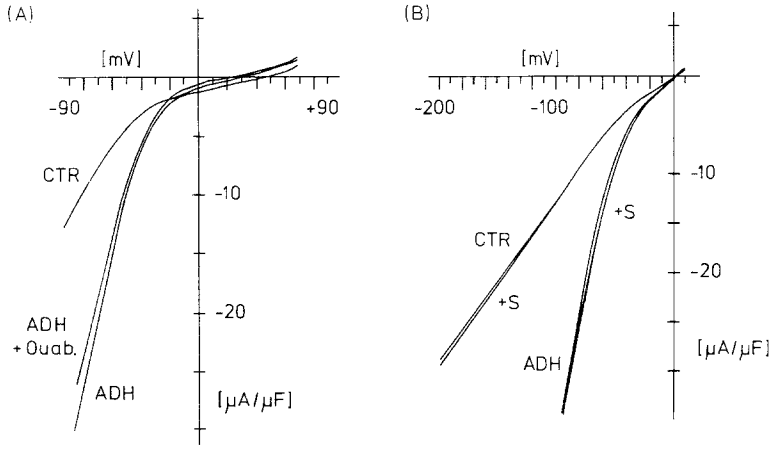

Fig. 1. Effect of oxytocin on the shunt I-V relationship of a K-depolarized toad bladder epithelium. Reference voltage is that of the serosal solution. Current flowing from the mucosal solution into the cells is positive. The command staircase started at positive voltages and decreased in steps of -5 mV (*A*) or -10 mV (*B*). Step duration was 5 msec. The smooth curves were obtained by connecting the data points by straight lines. (*A*): Mucosal solution was Na-free and contained 80 μM amiloride. The control curve (*CTR*) shows rectification of outward current, which occurred at less negative voltages, and was more pronounced, after exposure to oxytocin (*ADH*) for 64 min. Incubation with ouabain (10^{-3} M) for an additional 56 min did not significantly affect the shunt $I-V$ curve (*ADH + Ouab.*). (*B*): Mucosal solution was Na-free without amiloride. Abolition of the transepithelial osmotic gradient by addition of 60 mM sucrose (+*S*) to the mucosal solution for 3 min did not affect the rectification either before (*CTR*) or after exposure to oxytocin (*ADH*) for 25 to 35 min

computer program: I_{Na} was estimated for each voltage from the difference in current between the Na-transporting and the Na-free or fully amiloride-blocked states. P_{Na} and Na_c were calculated by fitting the I_{Na}-V curves with the constant field equation, as described previously for frog skin and toad bladder (Fuchs et al., 1977; Palmer et al., 1980). The Na_c-values thus obtained estimate Na activity in the cytoplasm close to the apical membrane.

To record current fluctuations, the chamber was shock-mounted on four springs and screened against 50-Hz pick-up. Aeration of the serosal solution was stopped during recording (5–10 min), but perfusion of the mucosal compartment was maintained at 30 ml/hr with air-equilibrated solution. The transepithelial voltage (V) was clamped with a low noise-feedback amplifier, with an input stage designed around a matched transistor pair (National Semi-conductor 2 N 4250) (Van Driessche & Lindemann, 1978). The short-circuit current was amplified with a gain of 50 mV/μA, fed through a high pass RC filter of 0.07 Hz characteristic frequency and amplified again (400-fold). The noise signal was then filtered with a steep cut-off at 140 Hz (antialiasing), amplified 2 to 10 times, and monitored on an oscilloscope. This signal was digitized by the A/D converter of the minicomputer at intervals of 2.44 msec for a period of 10 sec. The resulting time-series array of 4096 data points was subjected to a fast Fourier transform after which the current power density was computed on place. Ten to 20 power density spectra obtained sequentially were averaged. Data points were reduced further by averaging in intervals along the frequency axis. Equal point densities per decade of frequency were thus obtained at high frequencies, (*cf.* Fig. 4). The averaging process was continuously monitored on a $x-y$ display during the experiment. I_{sc} was also sampled.

The analysis of amiloride-induced shot-current noise was based on a single-channel model allowing for only two conductive states (open and fully closed). After evaluation of the apparent microscopic amiloride on and off-rate constants, k'_{02} and k'_{20}, from corner frequencies (f_c^A) [Appendix A, Eq. (A1)], the parameter i was estimated from the plateau values of the Lorentzian power density spectra and the macroscopic current, I_{Na} (*see* Appendix A). Subsequently, the area density of amiloride-accessible, electrically detectable channels (N_0+N_2) was obtained from the Lorentzian plateaus. $N_0 = I_{Na}/i$ was then calculated with I_{Na} values obtained at $A_o = 0$ and $Na_o = 60$ mM. The area density ($N = N_0 + N_1 + N_2$) of all electrically detectable Na channels was estimated by dividing N_0 by the steady-state probability (P_0) of a channel to be in the unblocked state in the absence of amiloride, $(1 + Na_o/K_N)^{-1}$, or by extrapolation of ($N_0 + N_2$) to infinite amiloride concentrations.

Results are expressed as means ± SEM unless indicated otherwise.

Results

Effects on Shunt-Conductance

In anuran skin and urinary bladder, antidiuretic hormone stimulates Na transport and increases the permeability of the epithelium to water and nonelectrolytes, e.g., urea (Andreoli & Schafer, 1976). One question addressed in the present report concerns possible effects on transcellular or paracellular ion-conducting pathways in parallel to the apical Na channels. It was necessary to deal with this question because we used the shunt I-V curves to calculate the I_{Na}-V relationship.

As shown in Fig. 1, the shunt conductance of K-depolarized preparations was increased by oxytocin but the increase was not the same at all voltages. At 0 mV the hormone raised the slope conductance by 10 to 100%, but as the initial conductance was usually small in this voltage range, the absolute increase was unimpressive. However, even in cases where the slope conductance near 0 mV was affected very little, the slope conductance at negative voltages was increased dramatically by oxytocin (Fig. 1*A* and *B*). Furthermore, the voltage range of

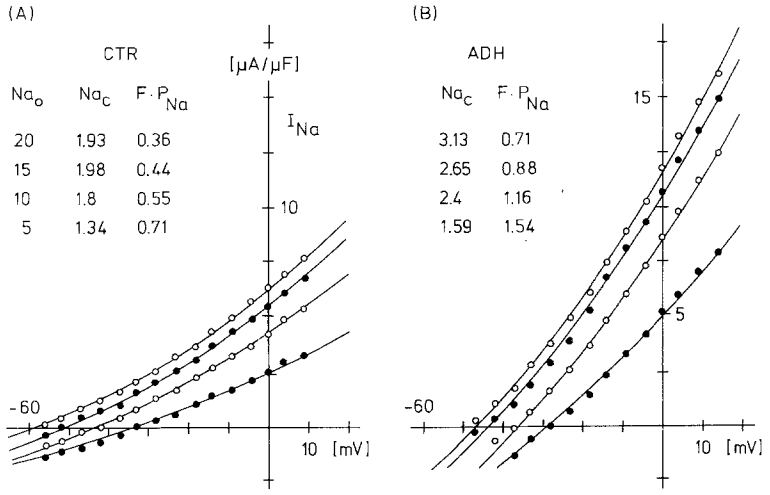

Fig. 2. Voltage dependence of I_{Na} at 20, 15, 10 and 5 mM Na_o. Shunt $I-V$ curves were obtained immediately after the total $I-V$ curves at each Na activity in the presence of 80 μM amiloride. I_{Na} was computed by subtracting the shunt current from the total current at each staircase voltage. The solid lines represent fits with the constant field equation which yielded the P_{Na} and Na_c values shown in the figure, in units of $cm \cdot sec^{-1} \cdot C \cdot mole^{-1}$ and mM, respectively. I_{Na} curves were obtained before (*A*) and after (*B*) stimulation by oxytocin for 32 to 60 min

transition from low to high slope conductance (i.e., the "breakpoint") was shifted to less negative voltages, i.e., in the same direction as the shift caused by K-depolarization of the basal-lateral membrane (Palmer et al., 1980).

Since the bathing solutions used in these experiments provided a small osmotic gradient across the epithelium, the effects leading to the oxytocin-dependent increase in conductance could have been mediated by cellular swelling. Addition of 60 mM sucrose to the mucosal solution, and its subsequent removal, however, did not affect the shunt I-V curve, before or after stimulation by oxytocin (Fig. 1*B*). An increase in cell volume therefore is not likely to be instrumental in the conductance change. The shunt I-V curve was not significantly changed after inhibition of active Na transport by ouabain (Fig. 1*A*), indicating that the observed "breakpoint" does not shift with the activity of the Na-K pump. A similar rectification behavior was observed in the shunt I-V curve of frog skin epithelium with K_2SO_4 solutions on both sides of the epithelium (Fuchs et al., 1977). This behavior may reflect the voltage dependence of the transapical K conductance.

Effect on Apical Na Transport

Addition of oxytocin to the serosal medium (high K-sucrose) increased I_{sc} after a delay of 2 to 5 min; the effect reached a maximum in about 30 min and persisted for at least 1 hr. I_{Na}-V curves were obtained at various values of Na_o as described in "Methods" and analyzed by fitting with the constant field equation.

After stimulation of I_{Na} by oxytocin, the fidelity of the fit with the constant field equation was maintained as shown in Fig. 2. Oxytocin raised P_{Na} and Na_c at all Na_o values. The increase in P_{Na} correlated closely ($r=0.99$) with the stimulation of I_{Na} at 0 mV (i.e., the Na component of I_{sc}) (Fig. 3). In 16 experiments, the relative oxytocin-dependent changes, observed in the presence of 20 mM Na_o, were I_{Na}: 1.64 ±0.10, P_{Na}: 168 ±0.11, Na_c: 1.31 ±0.07. A predominant hormonal stimulation of the pump activity should decrease Na_c. Therefore, the increase in P_{Na} combined with a significant increase in Na_c implies that in K-depolarized epithelia, the natriferic effect of oxytocin is based predominantly on a stimulation of Na entry through the apical membranes.

Effect on Na Self-Inhibition

In the toad bladder, as in frog skin, the dependence of I_{Na} on Na_o exhibits saturation kinetics (Frazier, Dempsey & Leaf, 1962). This feature is maintained after K-depolarization (Fig. 3*A*). In frog skin, I_{Na}-V analysis has shown that the saturation of I_{Na} is due to a decrease in P_{Na} with increasing Na_o at near constant Na_c (Fuchs et al., 1977). The Na_o-dependence of P_{Na} was described by

$$P_{Na} = P_{max}(1 + Na_o/K_N)^{-1} \quad (1)$$

where P_{max} is the maximal permeability found by extrapolation to $Na_o = 0$ and K_N the value of Na_o at half-maximal P_{Na}, i.e., the apparent inhibition constant of the Na-transport block by Na. P_{max} and K_N were obtained by plotting $1/P_{Na}$ against Na_o and calculating the regression line. We applied the same analysis to toad bladder data obtained before and after exposure to oxytocin, as shown in Fig. 3*B*.

Simultaneous changes of P_{Na} and Na_c in response to increasing Na_o are shown in Fig. 3*C*. It can be seen that the Na_c values, as found from reversal potentials of I_{Na}, vary between 1.5 and 3 mM. In view of these small changes and the previous results

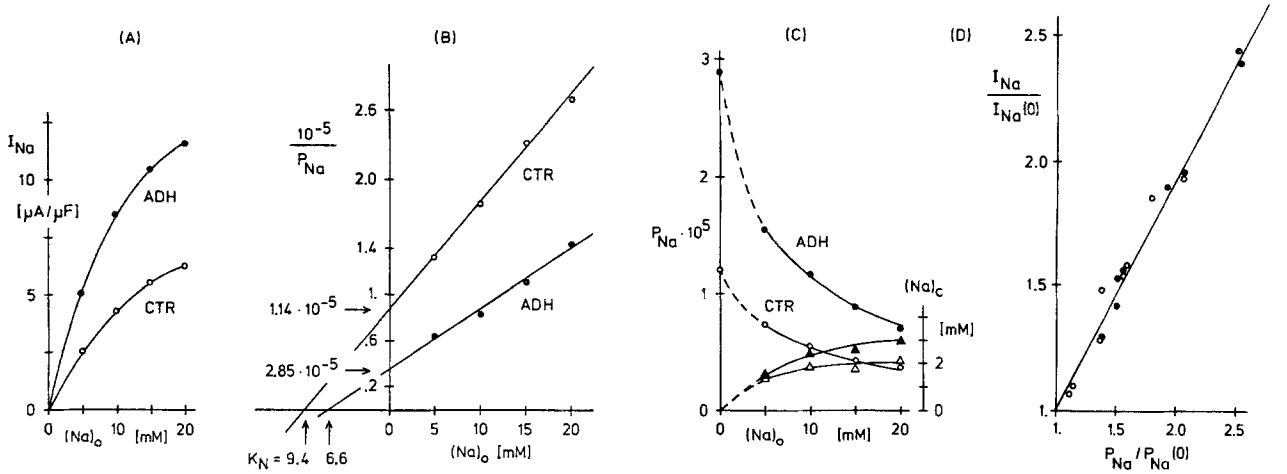

Fig. 3. Dependence of I_{Na}, P_{Na} and Na_c on Na_o. Measurements were made with a single hemibladder at $Na_o = 5$, 10, 15 and 20 mM. At each Na_o, total and shunt I-V curves were recorded both before (*CTR*) and 30–60 min after (*ADH*) addition of oxytocin, and steady-state values of I_{Na}, P_{Na} and Na_c were calculated. (*A*): Saturation of I_{Na} with increasing Na_o. Oxytocin increased I_{Na} at all values of Na_o without abolishing the saturation behavior. (*B*): Plot of $1/P_{Na}$ *vs.* Na_o. The regression lines yielded the indicated values of P_{max} (intercept with the ordinate) and K_N (intercept with the abcissa). (*C*): Decrease of P_{Na} (circles) and corresponding increase of Na_c (triangles) with increasing Na_o. P_{max} values, indicated at $Na_o = 0$, were obtained from regression lines (*B*). (*D*): Correlation of the relative increases in I_{Na} and P_{Na}. The ratios of steady-state values with $Na_o = 20$ mM before and during hormonal stimulation in 16 hemibladders are plotted. The slope of the regression line is 0.93, $r = 0.99$

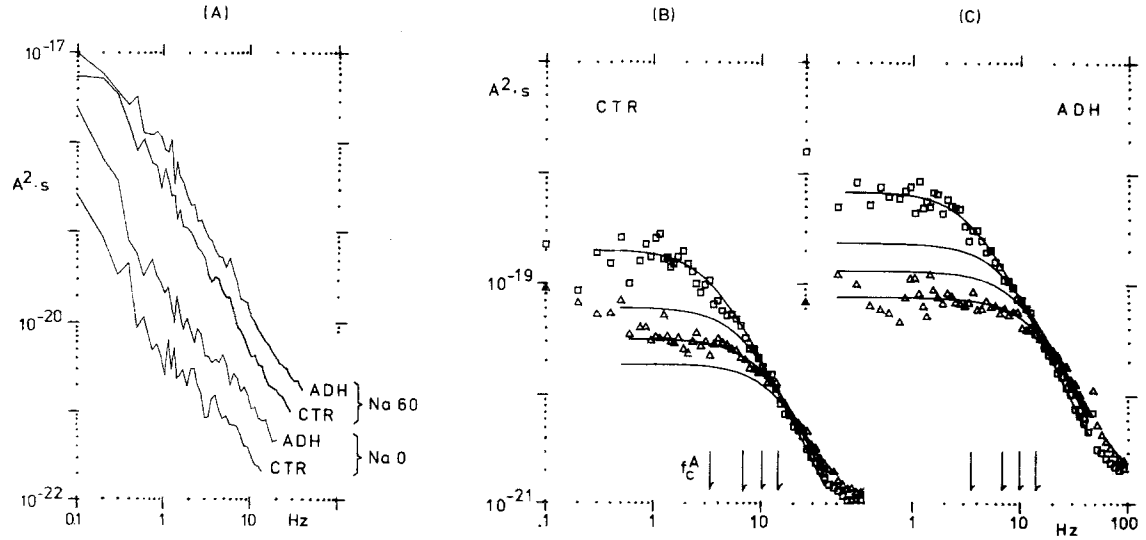

Fig. 4. Current power density spectra from toad bladder epithelia depolarized with high serosal K, and voltage clamped at $V = 0$ mV. Capacitance was 9 μF (*A*) and 6 μF (*B* and *C*). (*A*): Spectra in the absence of amiloride, with either $Na_o = 60$ mM or $Na_o = 0$ before (*CTR*) and 30–90 min after (*ADH*) addition of oxytocin. (*B*): Spectra obtained with $A_o = 1.2$ (□), 2.4, 3.6 (△) and 4.8 μM amiloride with $Na_o = 60$, before addition of oxytocin. Solid lines represent fits with Lorentzians. For clarity, data points of two spectra are omitted. (*C*): Spectra from the same hemibladder as in *B*, taken 30 to 90 min after the addition of oxytocin. The plateau power densities increased but the corner frequencies (arrows) were similar to those in *B*

of Palmer et al. (1980) it seems unlikely that the Na-dependence of P_{Na} is mediated by changes in Na_c, although a contribution from such a mechanism is not ruled out.

Oxytocin increased P_{max} by a factor of 2.12 ± 0.23 ($n = 15$). A substantial variation was observed in the values of K_N: In 15 control hemibladders K_N was 17 ± 5 mM ($\pm$SD). Oxytocin decreased K_N by a factor of 0.65 ± 0.06. In no experiment was an increase in K_N observed. Fig. 3*D* shows clearly that the increase in P_{Na} caused by oxytocin is not a consequence of abolition of the Na_o-dependence of P_{Na}.

Power Density Spectra and Rate Constants

Current fluctuations were recorded from K-depolarized bladders in the presence of 60 mM mucosal Na-activity. In the absence of amiloride, the current PDS computed from these fluctuations were steep; at high frequency the slopes were about -2 in double logarithmic plots (Fig. 4*A*). Some spectra showed

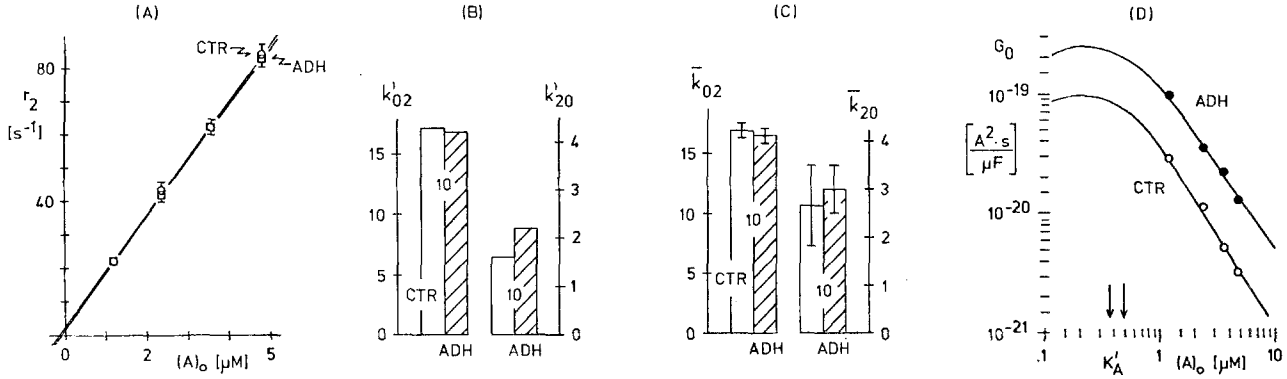

Fig. 5. Evaluation of amiloride-induced Lorentzian PDS. (*A*): Rate-concentration plot. $r_2 = 2\pi f_c^A$ plotted *vs.* A_o. Mean corner frequencies before (○) and after (□) addition of oxytocin were not significantly different. Bars indicate SEM of 10 experiments. (*B*): Apparent on-rate and off-rate constants (10^6 sec^{-1} M^{-1} and sec^{-1}, respectively) obtained from the mean corner frequencies (i.e., from the regression lines of *A*). (*C*): Means of the on- and off-rate constants of individual experiments. Bars indicate SEM of 10 experiments. (*D*). Plateau power density (G_0) plotted *vs.* A_0. The lines represent fits with Eq. (4), using $N = 0.22$ channels/10 fF, $i = 0.22$ pA for the control (○) and $N = 1.07$, $i = 0.17$ for after stimulation with oxytocin (●). K'_A values are indicated by arrows. Data are from a single hemibladder

less negative slopes at lower frequencies (around 0.1 Hz) but did not become horizontal. Therefore, these spectra could not be evaluated in terms of Lorentzian plateaus and corner frequencies. Spectra taken at zero Na_o were of significantly lower power density and had slopes between 1.2 and 2.0. After addition of oxytocin, power densities increased both at $Na_o = 0$ and 60 mM (Fig. 4*A*). The power increase observed at $Na_o = 0$ probably reflects the oxytocin-dependent increase in the zero-voltage shunt conductance (*see* Section 1 of Results).

In the presence of mucosal Na the addition of amiloride in submaximal concentrations (A_o) increased the power of current fluctuations above about 1 Hz and decreased the power at lower frequencies, as previously described for frog skin epithelium (Lindemann & Van Driessche, 1977). The resulting spectra could be fitted with Lorentzians. Plateau powers decreased and f_c^A increased when A_o was made larger. After stimulation by oxytocin the Lorentzian plateau-powers obtained with the A_o increased (Fig. 4*B* and *C* and 5*D*), but f_c^A, indicated by the arrows, showed little change.

Rate-concentration plots of $2\pi f_c^A$ *vs.* A_o gave linear relationships in the range of 1–5 μM of A_o, in which the Lorentzians could be evaluated, as shown in Fig. 5*A*. At each A_o, the mean f_c^A of 10 experiments was used to calculate the two regression lines, and from them the apparent microscopic on- and off-rate constants for the Na-channel block by amiloride (Fig. 5*B*). The on-rate constant (k'_{02}) showed no change in response to oxytocin while the off-rate constant (k'_{20}) showed a small increase which led to an apparent increase of 40% in K'_A computed from k'_{20}/k'_{02}. However, no significant changes in response to oxytocin were noted when the rate-concentration plots of individual experiments were evaluated by a paired *t*-test. Figure 5*C* shows mean values obtained by averaging the rate constants of 10 experiments.

To obtain estimates of the macroscopic K_A (i.e., K_A^{ma}) at 60 mM Na_o, approximate values of Na permeability (P'_{Na}) were calculated from:

$$P'_{Na} = (I_{Na})_{V=0}/(F \cdot Na_o) \tag{2}$$

in which F is the Faraday constant. This equation will underestimate P_{Na} somewhat, as Na_c is neglected. However, Na_c should have been less than 2 mM, because I_{Na} was considerably depressed by amiloride (Palmer et al., 1980). Therefore, no more than a 3% error is expected. Na_o/I_{Na} was plotted against A_o and $F \cdot P'_{max}$ was obtained from the intercept of the regression line with the ordinate (Fig. 6*A*). P'_{max} represents the value of P_{Na} at 60 mM Na_o in the absence of amiloride. P'_{Na}/P'_{max} was then plotted against the log of A_o to obtain normalized dose-response curves as shown in Fig. 6*B*. Note that the A_o values used for the noise experiments are restricted to the high concentration range of the dose-response curve, as only these concentrations yield evaluable Lorentzians. In some experiments, K_A^{ma} was increased by oxytocin, as previously described by Cuthbert and Shum (1975). Overall (10 experiments), the increase was not statistically significant, however (Fig. 6*C*).

The mean K_A^{ma} values were larger than those of the corresponding microscopic constant K'_A. The discrepancy can be explained by competitive inhibition of amiloride binding by Na, which makes K_A^{ma} and K'_A to different degrees larger than the true microscopic K_A value. Expressions for K_A^{ma} and K'_A are given in Appendix A, where we derive the relationship:

$$K_N \simeq Na_o/(K_A^{ma}/K'_A - 1). \tag{3}$$

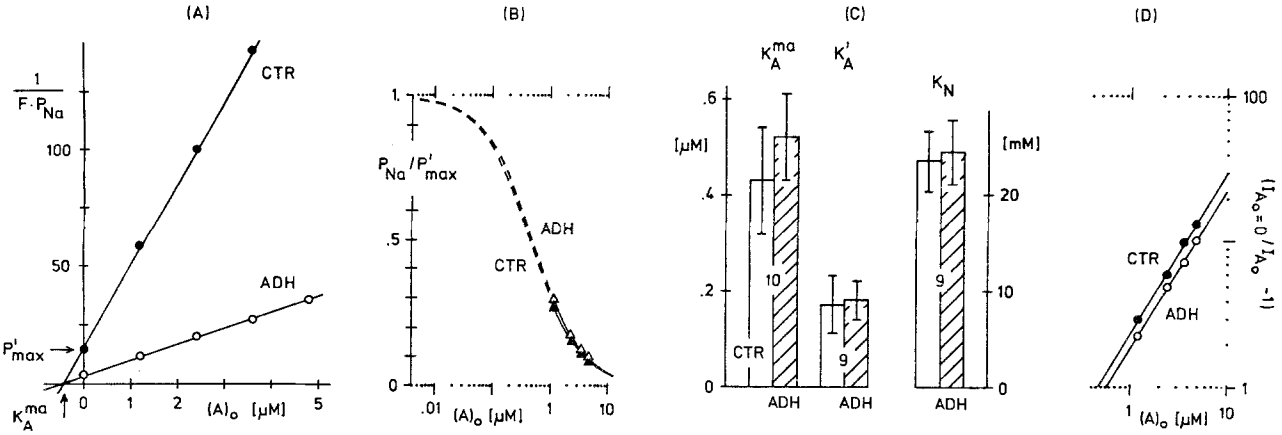

Fig. 6. (*A*): Linearized macroscopic dose-response curves of amiloride. I_{Na} values were recorded from a single hemibladder before (*CTR*) and 30–60 min after (*ADH*) addition of oxytocin. P'_{Na} values were estimated using Eq. (2) and $1/FP'_{Na}$ plotted *vs.* A_o. Intercepts on the ordinate and abscissa estimate P'_{max} and K_A^{ma}, respectively. K_A^{ma} was not affected by oxytocin, while P'_{max} was increased. (*B*): Dose-response curve of amiloride from the data shown in *A*. P'_{Na} values were normalized to P'_{max} and plotted *vs.* A_o. Only the high values of A_o used yielded evaluable Lorentzians. The dashed curves are extensions of the regression lines of *A*. (*C*): Inhibition constants obtained at 60 mM Na_o before (*CTR*) and after (*ADH*) addition of oxytocin. Values for the microscopic inhibition constant K'_A were obtained by averaging K'_A values obtained from the rate-concentration plots of individual experiments as in Fig. 5*C*. Values for K_N were obtained from Eq. (6) (*see* Fig. 8). Bars indicate SEM for 10 or 9 experiments. (*D*): Hill plots. $I_{A_o=0}$ and I_{A_o} are the Na currents in the absence and presence of amiloride. $(I_{A_o=0}/I_{A_o})-1$ was plotted *vs.* A_o. The Hill coefficients, measured as the slope of the regression lines in the log-log plot, were 1.07 ± 0.06 before (*CTR*) and 1.05 ± 0.03 during (*ADH*) stimulation with oxytocin (9 experiments)

As can be seen from this equation, a decrease in K_N would increase the ratio K_A^{ma}/K'_A. Indeed, the data from *I–V* curves revealed a 35% decrease in K_N after addition of oxytocin (e.g., Fig. 3*B*). When calculated from Eq. (3), however, based on the noise experiments, K_N was unaffected by the hormone (Fig. 6*C*). This discrepancy may be related to the fact that the noise experiments were done at threefold (or more) higher mucosal Na activities than were the *I–V* experiments.

Evaluation of Plateaus of Amiloride-Induced Lorentzians

At high concentrations of amiloride, Na uptake through the apical membrane is virtually nil even during ADH stimulation (e.g., Eigler, Kelter & Renner, 1967; Roloff, Dörge, Rick & Thurau, 1978). This means that a channel blocked by amiloride present in high concentrations will not pass Na ions. Furthermore, as shown in Fig. 6*D*, the Hill coefficient pertaining to amiloride in submaximal but high concentrations is close to unity, indicating that a stoichiometric ratio of one amiloride molecule per blocked channel will adequately fit the data. Accordingly, an "all-or-none" block model was used for the evaluation of amiloride-induced Lorentzians, as previously applied to frog skin (Lindemann & Van Driessche, 1977). The corresponding equations are detailed in Appendix A. The evaluation of spectral plateaus was always based on K'_A and r_2 values found from the regrssion line in the rate-concentration plot of the same experiment. Figure 5*D* depicts observed Lorentzian plateau values (G_0) as a function of A_o. The solid lines were calculated from

$$G_0 = 4\,N\,i^2\,(1/r_2)\,P_0\,P_2/(P_0+P_2) \qquad (4)$$

using values for A_o-dependent probabilities (P_0, P_2) and chemical rates (r_2) as detailed in Appendix A. It can be seen that the change in G_0 with A_o, as observed in K-depolarized bladders, conforms to the expectations of the all-or-none block model (Fig. 5*D*). In contrast, Van Driessche and Hegel (1978) reported that in nondepolarized toad bladders the change of G_0 with A_o is smaller than expected from a two-state blocking mechanism.

Channel Currents

Figure 5*D* shows that G_0 increases for a given amiloride concentration when the epithelium is stimulated with oxytocin. As the the effect of the hormone on K'_A and K_N was small (Fig. 6*C*), the occupancies P_0 and P_2 will have remained essentially unchanged. Therefore, the increase in G_0 can only be due to an increase in either N_0 or i, as shown by Eq. (4) after substituting N_0/P_0 for N.

Moreover, as I_{Na} depends linearly on N_0 and i (i.e., $I_{Na}=i\cdot N_0$) while G_0 depends linearly on N_0 but quadratically on i, a double-logarithmic plot of G_0 *vs.* I_{Na} should yield a slope of 1 if only N_0 is

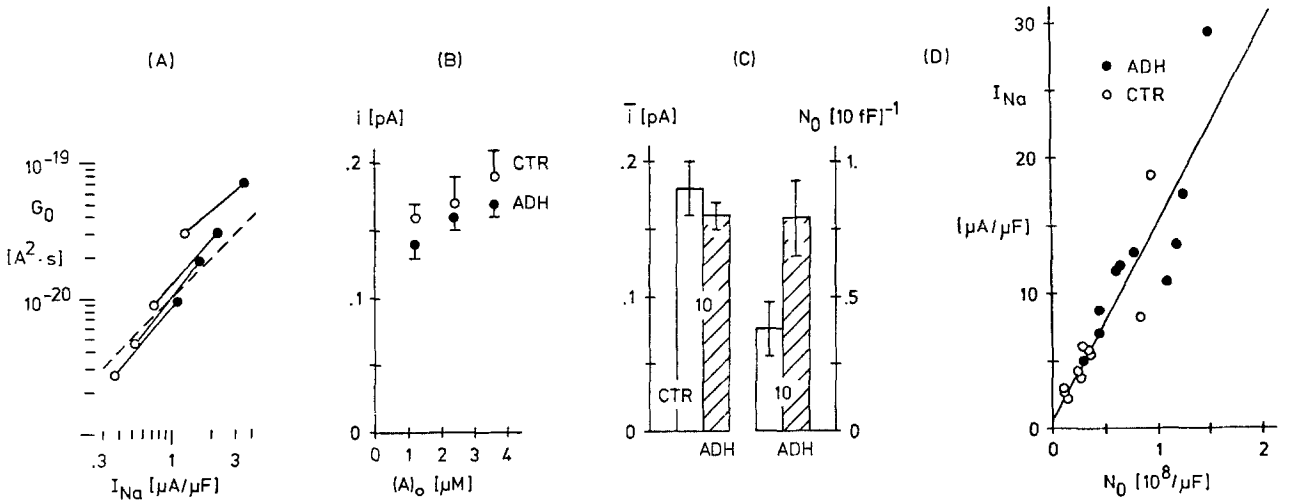

Fig. 7. Change of plateau power densities (G_0) with macroscopic Na current (I_{Na}). (*A*): Data were obtained from a single hemibladder at 4 amiloride concentrations before (○) and after (●) addition of oxytocin. Points from the same A_o are connected by straight lines. The dashed line indicates a slope of 1. The mean slope of 39 pairs of data points was 1.00 ± 0.06. (*B*): Variation of the shot current at different A_o before (○) and after (●) addition of oxytocin. Bars indicate SEM of 9 experiments. (*C*): Mean shot current (single-channel current). For each of 10 experiments values of i obtained at different A_o were averaged. The mean of these values ($\bar{i}$) was not significantly changed by addition of oxytocin (*ADH*). In contrast N_0 (calculated with Eq. (5*A*) for $A_o = 0$) was significantly increased. Bars indicate SEM of 10 experiments. (*D*): Correlation of I_{Na} with N_0. I_{Na} (at $Na_o = 60$ mM and $A_o = 0$) and N_0 were obtained before (○) and during (●) stimulation with oxytocin. The regression coefficient of the common regression line is 0.90. The slope indicates a mean channel current of 0.15 pA

increased, but a slope of 2 if only i is increased by the hormone. Figure 7*A* shows that the slope scatters around a value of 1. The mean slope was 1.00 ± 0.06 for 39 pairs of data points. This simple test implies that the natriferic effect of oxytocin involves predominantly an increase in N_0 rather than in i. Furthermore, with P_0 essentially constant, the increase in N_0 must be due to an increase in N.

When i was evaluated as indicated in the previous section and in appendix A, the values were higher at higher concentrations of amiloride; the change was barely significant (Fig. 7*B*). An increase of i with A_o may result from a decrease in Na_c which would increase the driving force for Na movement into the cell (*see* Discussion). This mechanism may also explain why i values obtained after stimulation of I_{Na} by oxytocin were slightly smaller than the controls (Fig. 7*B*), as oxytocin evoked an increase in Na_c (*cf.* Fig. 3*C*). As shown in Fig. 7*C*, oxytocin did not increase $\bar{i}$, the mean Na channel current averaged over all amiloride concentrations.

Area Densities

The area density of conducting channels can be obtained from:

$$I_{Na} = i \cdot N_0 \tag{5}$$

N_0 will, of course, depend on the Na and amiloride concentration used. The N_0 value in the absence of amiloride was calculated from:

$$N_0 = (I_{Na})_{A=0}/\bar{i} \tag{5a}$$

where $\bar{i}$ was calculated for each experiment. Figure 7*C* shows that the mean N_0 values increased strikingly in response to oxytocin. A plot of I_{Na}, at $A_o = 0$, against N_0 yielded a common regression coefficient of 0.90 and a slope of 0.15 pA/conducting channel, for the combined control and oxytocin data points (Fig. 7*D*). This value agrees reasonably well with that found by extrapolating i to $A_0 = 0$ (Fig. 7B).

N can be estimated by extrapolation, using Eq. (A6) derived in Appendix A, from a plot of $(N_0 + N_2)^{-1}$ *vs.* $(1 + A_o/K'_A)^{-1}$. If only amiloride blocked the channels, $(N_0 + N_2)$, should be independent of A_o because N_2 would only change at the expense of N_0. However, these plots are not horizontal as shown by the control line in Fig. 8*A*. This can be understood if Na and amiloride block channels competitively. In this case a subset of channels N_1 will be blocked by Na, and the subsets N_0 and N_2 will decrease accordingly. Equation (A6) predicts a slope of $(Na_o/K_N)/N$ and an intercept of $1/N$. K_N is obtained from the intercept of the regression line with the abscissa.

Plots based on Eq. (A6) are shown in Fig. 8*A*. Here the right data points (filled circles) of Fig. 8*A* represent $1/N_0$ values calculated for $A_o = 0$ according to Eq. (5*a*). They are close to the values predicted by the respective regression lines. Thus, the channel currents and channel densities computed for high A_o values from $\bar{i}$, based on the assumption of all-or-

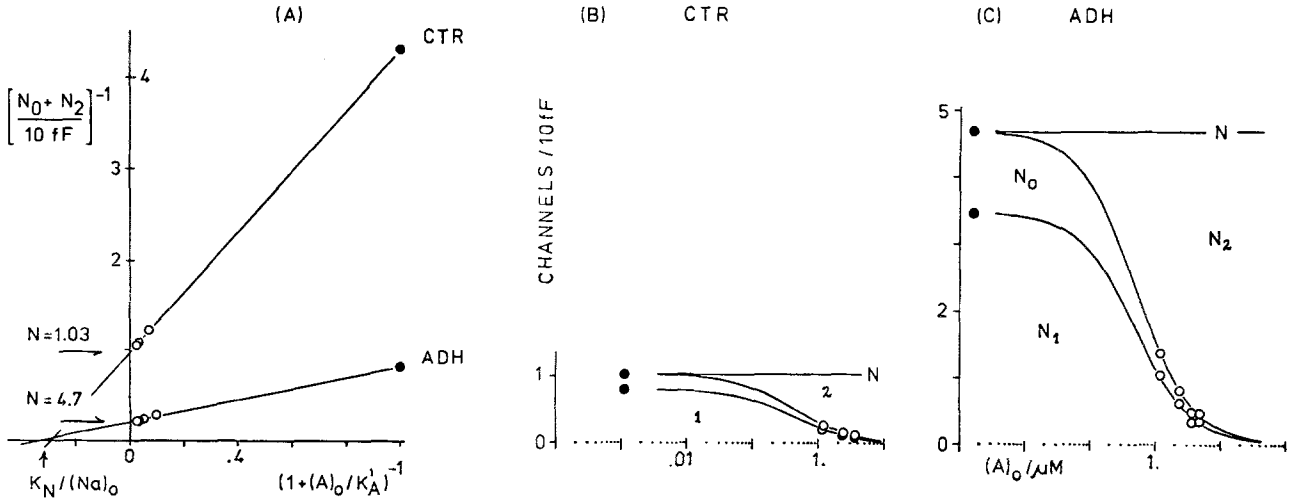

Fig. 8. (*A*): Plot of the inverse area density of amiloride-blockable channels *vs.* a function of A_o (*see* Eq. (6)). Data were obtained from a single hemibladder before (*CTR*) and during (*ADH*) stimulation with oxytocin. The regression lines were calculated from the data points obtained both at high A_o values (○) and at $A_o=0$ (●). For the latter points, $N_0+N_2=N_0$ was estimated from $I_{Na}/\bar{i}$. For all data points $\bar{i}$ values from this experiment were used. (*B*): Data from the control hemibladder in *A* replotted as conventional dose response curves to depict more clearly the distribution of N into N_0, N_1 and N_2. The filled circles represent values at $A_o=0$. The solid lines indicate the calculated dose-response curves for N_1 (lower curve), N_1+N_0 (upper curve), and $N_1+N_0+N_2=N$ (horizontal line) using values for N, K_N and K'_A obtained in this experiment. (*C*): Data from the hemibladder in *A* during stimulation with oxytocin, plotted as in *B*. It can be seen that the hormone increased both N_0 and N_1

none blocking behavior of amiloride, are consistent with the values of I_{Na} recorded in the absence of amiloride.

In a representative experiment shown in Fig. 8*A*, N increased from 1.03 to 4.7 Na channels per 10 fF on exposure to oxytocin and the density of Na-blocked channels increased from 0.77 to 3.45 channels per 10 fF, whereas P_1 remained practically invariant. The channel densities were also plotted more conventionally as a function of A_o in Fig. 8*B* and *C*. It can be seen that the increase in N_0 observed after exposure to oxytocin was not at the expense of N_1. Rather, the total area density N of electrically detectable Na channels increased. This inference is in accord with the results summarized for all experiments in Figs. 6*C* and 7*C*, which show a significant increase in N_0 with no change in K_N.

Discussion

The natriferic action of ADH was first described in amphibian skin and explained by an increase in Na transport through the outward facing diffusion barrier (e.g., Jörgensen, Levi & Ussing, 1946; Andersen & Ussing, 1957). This effect was also observed in toad urinary bladder (Frazier et al., 1962). Curran, Herrera and Flanigan (1963) inferred from a three-compartment tracer analysis in frog skin that the hormone increases the rate constant for uptake of Na at the outward facing barrier and in consequence the Na transport pool. The conclusion that ADH modulates apical permeability to Na in tight amphibian epithelia has been presented in numerous publications (for reviews *see* Andreoli & Schafer, 1976; Macknight, DiBona & Leaf, 1980). Our results confirm the stimulatory effect of ADH at the apical barrier; oxytocin increases P_{Na} and I_{Na} proportionately.

In frog skin, Cereijido, Herrera, Flanigan and Curran (1964) obtained evidence that P_{Na} is down-regulated with increasing Na_o. Concentration jump experiments indicated that this effect is predominantly due to Na_o rather than to Na_c (Fuchs et al., 1977). Van Driessche and Lindemann (1979) found that a decrease in the area density of conducting channels is the basis of the phenomenon of self-inhibition. This raises the possibility that ADH increases P_{Na} by release from inhibition by Na_o. Our I-V data do not support this possibility, however, because the relative increase in P_{Na} elicited by oxytocin was about the same at all values of Na_o, and K_N was not increased. This result agrees with similar observations of Frazier et al. (1962), Biber and Cruz (1973), and Mandel (1978) made with nondepolarized preparations.

The evaluation of amiloride-induced shot-noise provides further information on the basis of the hormone-dependent change in P_{Na}. Estimation of i and N_0, based on a two-state all-or-none block model, shows that i is not significantly increased by oxytocin, whereas N_0 increases in proportion to the increase in I_{Na} and, by inference, P_{Na}. In addition, K_N,

the Na inhibition constant, is not affected by oxytocin, implying a proportionate increase in the population of Na-blocked and Na-transporting channels. Thus the hormone, acting via cyclic AMP, converts nontransporting Na channels into transporting channels. This "recruitment" is the basis of the natriferic effect.

Our previous results indicated that P_{Na} is dependent on energy metabolism (Palmer et al., 1980). The possibility arises, therefore, that hormonal and metabolic control of P_{Na} share a terminal step (*see also* Palmer, Li, Lindemann & Edelman, 1982).

Channels could be recruited from cytoplasmic sources such as tubular structures or granules, which have access to the apical surface by fusion (Wade, 1978; Muller, Kachadorian & DiScala, 1980; Gronowicz, Masur & Holtzman, 1980). ADH increases the apical electrical capacitance as expected from addition of membrane area to the apical surface (Cuthbert & Painter, 1969; Warncke & Lindemann, 1980; Stetson, Lewis & Wade, 1981). While these processes may relate only to the hydroosmotic action of ADH (Kachadorian et al., 1977; Gronowicz et al., 1980; Stetson et al., 1981), the possibility remains that Na channels could be inserted into the apical membrane by a similar mechanism.

Alternatively, channels could be recruited from a pool of inactive units (N_x) already resident in the membrane. Indeed, in support of this hypothesis, Palmer and Edelman (1981) found that exposure of the apical surface to the protein modifying agent, diazosulfanilic acid, blocked both the baseline I_{sc} and subsequent stimulation by vasopressin to the same extent. Since the analogue diiododiazosulfanilic acid has the same effect on transport, and is impermeant (Ekblad, Strum & Edelman, 1976), this finding implies that N_x is in contact with the mucosal solution.

Should inactive channels also bind amiloride, our results would be in accord with the conclusion of Cuthbert and Shum (1975), and Cuthbert (1976) that antidiuretic hormone does not increase the number of amiloride-binding sites but prolongs the "open-time" of the channels. Estimates of channel densities by noise analysis in frog skin are about 1/2 to 1/6 of those found by binding of the high affinity amiloride analogue benzamil (Lindemann & Van Driessche, 1977; Aceves, Cuthbert & Edwardson, 1979). It seems possible, therefore, that the binding-method measures $N + N_x$.

In the toad bladder noise analysis yields an estimate of N_0 of one channel per 10 fF. This amounts to approximately 600 electrically detectable channels per cell, computed from estimates of the number of granular cells and apical membrane area per cell (DiBona, 1978). In contrast, Cuthbert and Shum (1975) found 3.6×10^5 amiloride binding sites per isolated toad bladder cell.

The single-channel currents computed from amiloride-induced shot-noise in toad bladder at large A_o are somewhat smaller than those previously observed with frog skin (Van Driessche & Lindemann, 1979). At moderate transapical driving forces, corresponding to about 50 mV, translocation rates in toad bladder were above 10^6 Na ions per sec per open channel in agreement with the values found for frog skin.

The dependence of i on amiloride concentration, indicated in Fig. 7*B*, deserves some comment. Such relationships are sometimes taken to indicate multistate blocking (Begenisich & Stevens, 1975) if more trivial explanations can be excluded. In our experiments, the recorded shot-noise current would decrease with decreasing blocker concentration (as is observed) if the K-depolarized basal-lateral membrane retained a significant resistance, making the intracellular potential positive during current flow. We show in Appendix B that the resistance would have to be 1/4 of the apical resistance or more to explain the variation of i with A_o. However, according to impedance measurements the fractional basal-lateral resistance is much smaller than 1/4 in K-depolarized toad bladders, excluding this explanation (Warncke & Lindemann, 1980). Another possibility is that at low A_o the increase in Na current increased Na_c, thus decreasing the chemical gradient across the apical membrane. While our I–V results do not show a large variation of Na_c at low Na_o, at the higher Na_o values used in the noise experiments larger changes in local Na_c may occur, due to concentration polarization effects at one or both surfaces of the apical membrane. Thus i would decrease with increasing I_{Na}, particularly when the channels are not distributed randomly, but cluster.

In summary, our results provide evidence that the stimulation of transepithelial Na transport by antidiuretic hormone is mediated by an increase in P_{Na} achieved by recruitment of Na channels from an electrically silent pool. The recruited channels are indistinguishable from those which function in the absence of the hormone, in their Na transport properties as well as in their interactions with amiloride and mucosal Na ions. In general the channel number, rather than the open channel translocation rate or gating rate, is the variable used in hormonal regulation of apical Na transport. We show in a subsequent paper that aldosterone also increases N_0 with no change in i (Palmer et al., 1982).

Financial assistance was provided by the Deutsche Forschungsgemeinschaft through SFB 38, project C-1 and by grants-in-aid from the United States Public Health Service (NIAMDD Grant

No. AM-13659 and NHLBI Grant No. HL-s3115). L.G.P. was recipient of a United States Public Health Service Traineeship (Grant No. AM-07219).

Appendix A

If Na ions and amiloride molecules competitively block conducting Na channels according to

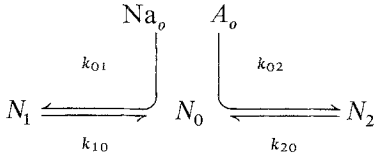

the inhibition constants with only one blocker present will be

$$K_N = k_{10}/k_{01} \quad \text{and} \quad K_A = k_{20}/k_{02}.$$

With

$$N = N_0 + N_1 + N_2$$

the occupational proabilities are

$$P_0 = (1 + \mathrm{Na}_o/K_N + A_o/K_A)^{-1} = N_0/N$$
$$P_1 = P_0 \cdot \mathrm{Na}_o/K_N = N_1/N$$
$$P_2 = P_0 \cdot A_o/K_A = N_2/N.$$

A double-Lorentzian power density spectrum is expected from this reaction scheme (*see* Lindemann & Van Driessche, 1978). If the two corner frequencies are sufficiently different in magnitude, and if pseudo-first order conditions hold, we obtain, for $A_o \gg K_A$,

$$r_2 = k_{02} A_o + k_{20} + k_{01} \mathrm{Na}_o = 2\pi f_c^A. \tag{A1}$$

Therefore, a rate-concentration plot of r_2 versus A_o yields a slope of k_{02} and an ordinate intercept of

$$k'_{20} = k_{20} + k_{01} \mathrm{Na}_o.$$

Only at low k_{01} (*see* Van Driessche & Lindemann, 1979) will the intercept estimate k_{20}. The apparent K_A value obtained from this plot will be

$$K'_A = K_A[1 + k_{01} \mathrm{Na}_o/k_{20}]$$

i.e., close to the true K_A if k_{01} is small. On the other hand, the macroscopic inhibition constant of amiloride is

$$K_A^{ma} = K_A \cdot (1 + \mathrm{Na}_o/K_N).$$

With $k_{20} > k_{10}$, K_A^{ma} will be larger than K'_A. In this case the ratio of the two inhibition constants:

$$\frac{K_A^{ma}}{K'_A} = \frac{1 + \mathrm{Na}_o/K_N}{1 + (k_{10}/k_{20})(\mathrm{Na}_o/K_N)} \tag{A2}$$

permits the estimation of K_N, using:

$$K_N \simeq \mathrm{Na}_o/(K_A^{ma}/K'_A - 1). \tag{A3}$$

Of the two Lorentzian plateaus, the one expected at higher frequencies will be of power density

$$G_0 = 4 N i^2 (1/r_2) P_0 P_2/(P_0 + P_2)$$
$$= 4 N i^2 \left(\frac{A_o}{K_A}\right) \Big/ \left(k_{20} \cdot \left(1 + \frac{A_o}{K_A}\right)^2 \cdot \left(1 + \frac{\mathrm{Na}_o}{K_N} + \frac{A_o}{K_A}\right)\right). \tag{A4}$$

After substitution with

$$I_{\mathrm{Na}} = i \cdot N \cdot P_0 \tag{A5}$$

which is justified only if the blocking is all or none, such that the shot-current is identical with the single-channel Na current, we obtain

$$G_0 = 4 i I_{\mathrm{Na}} (1/r_2) P_2/(P_0 + P_2).$$

Further substitution with

$$P_2/(P_0 + P_2) = (A_o/K_A)/(1 + A_o/K_A)$$

and

$$r_2 \approx k_{20}(1 + A_o/K_A)$$

yields

$$G_0 = 4 i I (A_o/K_A)/[k_{20} \cdot (1 + A_o/K_A)^2]$$

from which i can be determined. Subsequently, N_0 can be calculated from $N_0 = I_{\mathrm{Na}}/i$ for a given Na_o and A_o. Furthermore, if K_N is known

$$\frac{(N_0)_{A_o}}{(P_0)_{A_o}} = \frac{(I_{\mathrm{Na}})_{A_o}}{i}\left(1 + \frac{\mathrm{Na}_o}{K_N} + \frac{A_o}{K_A}\right)$$

will estimate the area density of all electrically detectable channels. Alternatively, the area density of amiloride accessible channels $(N_0 + N_2)$ at a given Na_o and A_o may be found from

$$N_0 + N_2 = N_0(1 + A_o/K_A) = \frac{(I_{\mathrm{Na}})_{A_o}}{i}(1 + A_o/K_A).$$

Substitution with

$$N_0 = N \cdot \left(1 + \frac{\mathrm{Na}_o}{K_N} + \frac{A_o}{K_A}\right)^{-1}$$

yields

$$(N_0 + N_2)^{-1} = \frac{1}{N} + \frac{1}{N}\frac{\mathrm{Na}_o}{K_N}\left(1 + \frac{A_o}{K_A}\right)^{-1} \tag{A6}$$

from which N can be estimated by plotting $(N_0 + N_2)^{-1}$ versus $(1 + A_o/K_A)^{-1}$ and extrapolating to infinite A_o, as shown in Fig. 8*A*.

Appendix B

The effect of a significant basolateral membrane resistance R_b on the recorded shot-current i_{clamp} is evaluated. For a short-circuited two-membrane preparation of negligible series resistance the transapical membrane voltage is

$$V_a = E_a \cdot R_b/(R_a + R_b)$$

in which E_a and R_a stand for reversal potential and resistance of the apical membrane. The reversal potential of the basolateral membrane is taken to be 0 mV in the K-depolarized state (*compare* Eq. (19) in Lindemann & DeFelice, 1981). We suppose for simplicity that the apical membrane is ideally selective for Na ions; its N Na channels are blocked randomly by amiloride and have resistance r_{ch} in the open state, such that

$$i = (V_a - E_a)/r_{ch}$$

and

$$R_a = (1 + A_o/K_A^{ma}) \cdot r_{ch}/N.$$

By substitution we obtain for the shot-current

$$i = \frac{-E_a}{r_{ch}} \cdot \frac{R_a}{R_a + R_b}.$$

The recorded shot-current will be given by

$$i_{clamp} = i \cdot R_a/(R_a + R_b).$$

This relationship pertains to zero frequency. For corrections at all frequencies *see* Lindemann and De Felice (1981). By substitution we obtain with $r_{ch}/N = R_a^{A_o=0} i_{clamp}$ as a saturating function of A_o:

$$i_{clamp} = \frac{-E_a}{r_{ch}} \cdot \left(\frac{R_a^{A_o=0} \cdot (1 + A_o/K_A^{ma})}{R_b + R_a^{A_o=0} \cdot (1 + A_o/K_A^{ma})} \right)^2$$

and

$$i_{clamp}^{A_o=0} = \frac{E_a}{r_{ch}} \left(\frac{R_a^{A_o=0}}{R_b + R_a^{A_o=0}} \right)^2.$$

We take the ratio of these two clamp-currents and find with the abbreviation $\beta = \sqrt{i_{clamp}/i_{clamp}^{A_o=0}}$

$$\frac{R_b}{R_a^{A_o=0}} = \frac{(1 + A_o/K_A^{ma})(\beta - 1)}{(1 + A_o/K_A^{ma}) - \beta}.$$

In Fig. 7*B* we find for $i_{clamp}^{A_o=0}$ about 0.12 pA (or less when the nonlinearity of the relationship is taken into account) and with $K_A^{ma} = 0.5\,\mu M$ for $A_o = 3.7\,\mu M$ about 0.18 pA. For this pair of clamp currents $\beta = 1.223$ and $R_b/R_a^{A_o=0} = 0.26$. For smaller values of $i_{clamp}^{A_o=0}$ the ratio will be even larger.

References

Aceves, J., Cuthbert, A.W., Edwardson, J.M. 1979. Estimation of the density of sodium entry sites in frog skin epithelium from the uptake of [^{3}H]-benzamil. *J. Physiol. (London)* **295**:477–490

Andersen, B., Ussing, H.H. 1957. Solvent drag on nonelectrolytes during osmotic flow through isolated toad skin and its response to antidiuretic hormone. *Acta Physiol. Scand.* **39**:228–239

Andreoli, T.E., Schafer, J.A. 1976. Mass transport across cell membranes: The effects of antidiuretic hormone on water and solute flows in epithelia. *Annu. Rev. Physiol.* **38**:451–500

Begenisich, T., Stevens, C.F. 1975. How many conductance states do potassium channels have? *Biophys. J.* **15**:843–846

Biber, T.U.L., Cruz, L.J. 1973. Effect of antidiuretic hormone on sodium uptake across outer surface of frog skin. *Am. J. Physiol.* **225**:912–917

Cereijido, M., Herrera, F.C., Flanigan, W.J., Curran, P.F. 1964. The influence of Na-concentration on Na-transport across frog skin. *J. Gen. Physiol.* **47**:879–893

Curran, P.F., Herrera, F.C., Flanigan, W.J. 1963. The effect of Ca and antidiuretic hormone on Na-transport across frog skin. II. Sites and mechanisms of action. *J. Gen. Physiol.* **46**:1011–1027

Cuthbert, A.W. 1976. Amiloride as a probe for sodium entry sites in frog skin epithelium. *J. Physiol. (London)* **266**:28P

Cuthbert, A.W., Painter, E. 1969. Capacitance changes in frog skin caused by theophylline and antidiuretic hormone. *Brit. J. Pharmacol.* **37**:314–324

Cuthbert, A.W., Shum, W.K. 1974. Amiloride and the sodium channel. *Naunyn Schmiederbergs Arch. Pharmacol.* **281**:261–269

Cuthbert, A.W., Shum, W.K. 1975. Effects of vasopressin and aldosterone on amiloride binding in toad bladder epithelial cells. *Proc. R. Soc. London B* **189**:543–575

DiBona, D.R. 1978. Direct visualization of epithelial morphology in the living amphibian urinary bladder. *J. Membrane Biol.* **Special Issue**:45–70

Eigler, J., Kelter, J., Renner, E. 1967. Wirkungscharakteristika eines neuen Acylquanidins-Amilorid-HCl (MK 870) an der isolierten Haut von Amphibien. *Klin. Wochenschr.* **45**:737–738

Ekblad, E.B.M., Strum, J.M., Edelman, I.S. 1976. Differential covalent labeling of apical and basal-lateral membranes of the epithelium of the toad bladder. *J. Membrane Biol.* **26**:301–317

Frazier, H.S., Dempsey, E.F., Leaf, A. 1962. Movement of sodium across the mucosal surface of the isolated toad bladder and its modification by vasopressin. *J. Gen. Physiol.* **45**:529–543

Fuchs, W., Hviid Larsen, E., Lindemann, B. 1977. Current-voltage curve of sodium channels and concentration dependence of sodium permeability in frog skin. *J. Physiol. (London)* **267**:137–166

Furhmann, F.A., Ussing, H.H. 1951. A characteristic response of the isolated frog skin potential to neurohypophyseal principles and its relation to the transport of sodium and water. *J. Cell. Comp. Physiol.* **38**:109–130

Gronowicz, G., Masur, S.K., Holtzman, E. 1980. Quantitative analysis of exocytosis and endocytosis in the hydroosmotic response of toad bladder. *J. Membrane Biol.* **52**:221–235

Jörgensen, C.B., Levi, H., Ussing, H.H. 1946. On the influence of neurohypophyseal principles on the sodium metabolism in the axolotl (*Amblystoma mexicanuum*). *Acta Physiol. Scand.* **12**:350–371

Kachadorian, W.A., Levine, S.D., Wade, J.B., DiScala, V.A., Hays, R.M. 1977. Relationship of aggregated intramembranous particles to water permeability in vasopressin-treated toad urinary bladder. *J. Clin. Invest.* **59**:576–581

Li, J.H.-Y., Palmer, L.G., Edelman, I.S., Lindemann, B. 1979. Effect of ADH on Na-channel parameters in toad urinary bladder. *Pfluegers Arch.* **382**:*R*13

Lindemann, B., DeFelice, L.J. 1981. On the use of general network functions in the evaluation of noise spectra obtained from epithelia. *In:* Ion Transport by Epithelia: Recent Advances. S.G. Schultz, editor. Raven Press, New York *(in press)*

Lindemann, B., Van Driessche, W. 1977. Sodium specific membrane channels of frog skin are pores: Current fluctuations reveal high turnover. *Science* **195**:292–294

Lindemann, B., Van Driessche, W. 1978. The mechanism of Na-uptake through Na-selective channels in the epithelium of frog skin. *In:* Membrane Transport Processes. J.F. Hoffman, editor. Vol. 1, p. 155. Raven Press, New York

Macknight, A.D.C., DiBona, D.R., Leaf, A. 1980. Sodium transport across toad urinary bladder: A model "tight" epithelium. *Physiol. Rev.* **60**:615–715

Mandel, L.J. 1978. Effects of pH, Ca, ADH, and theophylline on kinetics of Na-entry in frog skin. *Am. J. Physiol.* **235**:*C*35–*C*48

Muller, J., Kachadorian, W.A., DiScala, V.A. 1980. Evidence that ADH-stimulated intramembrane particle aggregates are transferred from cytoplasmic to luminal membranes in toad bladder epithelial cells. *J. Cell Biol.* **85**:83–95

Orloff, J., Handler, J. 1962. The similarity of effects of vasopressin, adenosine-3′,5′-phosphate (cyclic AMP) and theophylline on the toad bladder. *J. Clin. Invest.* **41**:702–709

Orloff, J., Handler, J. 1967. The role of adenosine 3′,5′-phosphate in the action of antidiuretic hormone. *Am. J. Med.* **42**:757–768

Palmer, L.G., Edelman, I.S. 1981. Control of apical Na permeability in the toad urinary bladder by aldosterone. *Ann. N.Y. Acad. Sci. (in press)*

Palmer, L.G., Edelman, I.S., Lindemann, B. 1980. Current-voltage analysis of apical sodium-transport in toad urinary bladders: Effects of inhibitors of transport and metabolism. *J. Membrane Biol.* **57**:59–71

Palmer, L.G., Li, J.H.-Y., Lindemann, G., Edelman, I.S. 1982. Aldosterone control of the density of sodium channels in the toad urinary bladder. *J. Membrane Biol.* **64**:91–102

Roloff, C., Dörge, A., Rick, R., Thurau, K. 1978. Effect of vasopressin on intracellular electrolyte composition of the frog skin. *Pfluegers Arch.* **377**:*R*40

Stetson, D.L., Lewis, S.A., Wade, J.B. 1981. ADH-induced increase in transepithelial capacitance in toad bladder. *Biophys. J.* **33**:43*a*

Van Driessche, W., Hegel, U. 1978. Amiloride induced fluctuations of short circuit current through toad urinary bladder. 6th International Biophysics Congress. Kyoto, Japan. p. 215

Van Driessche, W., Lindemann, B. 1978. Low noise amplification of voltage and current fluctuations arising in epithelia. *Rev. Sci. Instrum.* **49**:52–55

Van Driessche, W., Lindemann, B. 1979. Concentration dependence of currents through single sodium-selective pores in frog skin. *Nature (London)* **282**:519–520

Wade, J.B. 1978. Membrane structural specialization of the toad urinary bladder revealed by the freeze-fracture technique. III. Location, structure and vasopressin dependence of intramembrane particle arrays. *J. Membrane Biol.* **Special Issue**:281–296

Warnche, J., Lindemann, B. 1979. A sinewave-burst method to obtain impedance spectra of transporting epithelia during voltage clamp. *Pfluegers Arch.* **382**:*R*12

Warncke, J., Lindemann, B. 1980. Effect of ADH on the capacitance of apical epithelial membranes. *Proc. 28th Int. Congr. Physiol. Sci. (Budapest)* pp. 129–133.

Received 15 April 1981; revised 23 July 1981